

---

# Princeton Plasma Physics Laboratory

---

PPPL-

PPPL-



Prepared for the U.S. Department of Energy under Contract DE-AC02-09CH11466.

# Princeton Plasma Physics Laboratory

## Report Disclaimers

---

### Full Legal Disclaimer

This report was prepared as an account of work sponsored by an agency of the United States Government. Neither the United States Government nor any agency thereof, nor any of their employees, nor any of their contractors, subcontractors or their employees, makes any warranty, express or implied, or assumes any legal liability or responsibility for the accuracy, completeness, or any third party's use or the results of such use of any information, apparatus, product, or process disclosed, or represents that its use would not infringe privately owned rights. Reference herein to any specific commercial product, process, or service by trade name, trademark, manufacturer, or otherwise, does not necessarily constitute or imply its endorsement, recommendation, or favoring by the United States Government or any agency thereof or its contractors or subcontractors. The views and opinions of authors expressed herein do not necessarily state or reflect those of the United States Government or any agency thereof.

### Trademark Disclaimer

Reference herein to any specific commercial product, process, or service by trade name, trademark, manufacturer, or otherwise, does not necessarily constitute or imply its endorsement, recommendation, or favoring by the United States Government or any agency thereof or its contractors or subcontractors.

---

## PPPL Report Availability

### Princeton Plasma Physics Laboratory:

<http://www.pppl.gov/techreports.cfm>

### Office of Scientific and Technical Information (OSTI):

<http://www.osti.gov/bridge>

---

### Related Links:

[U.S. Department of Energy](#)

[Office of Scientific and Technical Information](#)

[Fusion Links](#)

# Generalized expression for polarization density

Lu Wang<sup>1,2</sup> and T.S. Hahm<sup>2</sup>

<sup>1</sup>School of Physics, Peking University, Beijing 100871, China

<sup>2</sup>Princeton University, Princeton Plasma Physics Laboratory

P. O. Box 451, Princeton, NJ 08543, USA

(Dated: April 16, 2009)

## Abstract

A general polarization density which consists of classical and neoclassical parts is systematically derived via modern gyrokinetics and bounce-kinetics by employing a phase-space Lagrangian Lie-transform perturbation method. The origins of polarization density are further elucidated. Extending the work on neoclassical polarization for long wavelength compared to ion banana width [M. N. Rosenbluth and F. L. Hinton, *Phys. Rev. Lett.* **80**, 724 (1998)], an analytical formula for the generalized neoclassical polarization including both finite-banana-width (FBW) and finite-Larmor-radius (FLR) effects for arbitrary radial wavelength in comparison to banana width and gyroradius is derived. In addition to the contribution from trapped particles, the contribution of passing particles to the neoclassical polarization is also explicitly calculated. Our analytic expression agrees very well with the previous numerical results for a wide range of radial wavelength.

## I. INTRODUCTION

Reduced kinetic equations have provided theoretical foundations for studying low-frequency microturbulence. When the frequency of the fluctuation  $\omega$  is much smaller than the cyclotron frequency  $\Omega = eB/(mc)$ , the fast gyroangle can be asymptotically removed from the governing equation, and the first adiabatic invariant  $\mu$  exists. For this case, nonlinear gyrokinetics from a conventional multiple-scale-expansion method was first presented by Frieman and Chen.<sup>1</sup> After that, modern nonlinear gyrokinetics based on a Lie-transform perturbation method, previously used by Littlejohn<sup>2-4</sup> to derive guiding-center (gc) equa-

tions, was developed and has been improved in recent years.<sup>5-14</sup> The classical polarization density plays an important role in gyrokinetic simulations.<sup>15</sup> Some detailed theoretical discussions of the classical polarization have been also presented.<sup>10,14</sup>

Furthermore, if the characteristic frequency  $\omega$  is even much smaller than the bounce (transit) frequency  $\omega_{b(t)}$ , there exists another adiabatic invariant  $J_{b(t)}$ , corresponding to the bounce motion of trapped particles (denoted by index b) or transit motion for passing particles (denoted by index t) in a nonuniform magnetic field. Based on the existence of this second adiabatic invariant, bounce-kinetics was derived by using a conventional multiple-scale-ordering expansion.<sup>16</sup> Like modern gyrokinetics, Lie-transform perturbation method was also used to derive bounce-guiding-center (bgc) equations without fluctuation<sup>17</sup>, then bounce-gyrocenter (bgy) kinetics with electrostatic<sup>18</sup> and electromagnetic fluctuations.<sup>19</sup> In this work, we consider the electrostatic case. The bounce-kinetic equations have been widely applied to analytic theories of trapped electron mode (TEM) turbulence,<sup>20-23</sup> and derivation of bounce-averaged fluid equations.<sup>24</sup> They are also used to derive neoclassical polarization shielding, and residual zonal flow.<sup>18,25-35</sup> Hinton and Robertson found that the dielectric constant is increased due to the neoclassical polarization drift.<sup>26</sup> Rosenbluth and Hinton (R-H) investigated collisionless zonal flow evolution<sup>27</sup> which is affected by neoclassical polarization. Later, Hinton and Rosenbluth then extended their work to include the effects of collisions.<sup>28</sup> The R-H residual zonal flow is believed to affect turbulence driven transport. For instance, it can upshift the effective threshold of ion temperature gradient (ITG) instability.<sup>29</sup> A favorable role of plasma shaping in reducing ion thermal transport in ITG simulations has been attributed to the effect of shaping on the R-H residual zonal flows,<sup>30-32</sup> while an additional change in the shearing effect<sup>36</sup> via Geodesic Acoustic Mode frequency has been mentioned as another possibility.<sup>32</sup> An analytic expression for the R-H residual flow with shaping effects has been derived for a model equilibrium.<sup>33</sup> Theoretical progress has then extended to more detailed calculations in helical systems by Sugama and Watanabe.<sup>34,35</sup>

However, all of the works above were based on an assumption, i.e., the radial wavelength are much larger than the ion poloidal gyroradius. Jenko et al., reported based on their gyrokinetic simulations, that the residual zonal flow level was enhanced at the short wavelengths in the electron temperature gradient (ETG) turbulence.<sup>37</sup> More recently, neoclassical polarization in the short wavelength regime has been studied by Xiao and Catto.<sup>38</sup> Follow-

ing R-H's approach,<sup>27,28</sup> they calculated the neoclassical polarization and residual zonal flow for somewhat shorter wavelengths analytically, and for arbitrary wavelengths numerically.<sup>38</sup> One often recognizes only the finite-banana-width (FBW) effects when he/she refers to the neoclassical polarization in the long wavelength limit. But, the finite-Larmor-radius (FLR) effects on the neoclassical polarization can no longer be ignored in the short wavelength regime. Hence, it is meaningful to derive analytically a generalized neoclassical polarization including the FLR as well as the FBW effects for arbitrary wavelength in comparison to gyroradius and poloidal gyroradius. The progress in gyrokinetics and bounce-kinetics and their applications to classical and neoclassical polarization shielding are summarized in Tables I and II.

In the present paper, we start from a particle phase-space Lagrangian and apply the Lie-transform perturbation method, transforming it into gyrocenter (gy) phase-space (gyrokinetics) and then from gy into bgy phase-space (bounce-kinetics). For bounce-kinetics, unlike Fong and Hahm<sup>18</sup> and Brizard<sup>19</sup> who started from the gc phase-space Lagrangian, we begin with the lowest-order gy phase-space Lagrangian and keep the FLR effects in the perturbed parts of the Lagrangian which were ignored in previous works. This is the key point of this work. In this way, we can obtain the classical and neoclassical polarization for arbitrary radial wavelengths simultaneously via two consecutive pull-back transformations and provide a clear interpretation of their origins. Another advantage of keeping the FLR effects in the perturbed parts of the Lagrangian is that we can obtain not only the FBW but also the FLR effects on the neoclassical polarization density, which is important in the short wavelength regime. We also take into account the contribution from the passing particles to the neoclassical polarization, which can be dominant in the short wavelength regime when  $\epsilon$  (the local revers aspect ratio) is extremely small. The procedures of gyrokinetics and bounce-kinetics illuminating the origins of classical and neoclassical polarization are presented in Fig. 1 and Fig. 2.

The principle results of this paper are as follows:

1. The general polarization density which consists of neoclassical and classical parts is systematically derived via pull-back transformation from bgy to bgc, then to gy, phase space, and from gy to gc, then to particle, phase space, respectively.

2. A generalized expression for the neoclassical polarization density including the FBW as well as the FLR effects, for arbitrary radial wavelength, is obtained simultaneously, which extends the R-H calculation in the long wavelength limit.<sup>27</sup>
3. Not only the contribution from the trapped particles, but also the passing particles' contribution, to the neoclassical polarization density is separately calculated.
4. Our analytic expression agrees well with the previous numerical results.<sup>37,38</sup>

The remainder of this paper is organized as follows. In Sec. II, the results of a phase-space Lagrangian transformation from particle phase space to gy, and then to bgy, phase space are presented. Both of them are subject to the two-step transformation scheme.<sup>8,13,19</sup> We systematically derive the general polarization density via a pull-back transformation in Sec. III. It decouples naturally into classical and neoclassical parts. The general polarization for arbitrary wavelength in comparison to gyroradius and poloidal gyroradius is calculated and compared with the previous numerical results<sup>37,38</sup> in Sec. IV. For the neoclassical part, we have considered the contributions from both the trapped and the passing particles in three limiting cases. In Sec. V, we summarize our work and discuss its possible applications. We focus our attention on the systematic derivation of the general polarization, and the calculation of the generalized neoclassical polarization, including both the trapped and the passing particles' contribution for arbitrary gyroradius and poloidal gyroradius.

## II. PHASE-SPACE LAGRANGIAN TRANSFORMATION FOR GYROKINETICS AND BOUNCE-KINETICS

In this section, we present the main results of the phase-space Lagrangian transformation for gyrokinetics and bounce-kinetics. We employ the Lie-transform perturbation method in the present work. For a systematic derivation of a general polarization density which includes both FLR and FBW effects, we pursue a two-step transformation scheme<sup>8,13,19</sup> for both gyrokinetics and bounce-kinetics. The transformation for the decoupling gyroangle dependence in gyrokinetics starts from the particle phase-space Lagrangian. From the gc transformation of the unperturbed particle phase-space Lagrangian, the unperturbed gc phase-space Lagrangian is obtained. The gy transformation on the fluctuations leads to the gy phase-

space Lagrangian. For bounce-kinetics, starting from the gy phase-space Lagrangian, we first perform a bgc phase-space transformation on the equilibrium (zeroth order) part of it. Then we complete the bgy phase-space transformation on the perturbed part of the bgc phase-space Lagrangian which includes the FLR effects. These phase-space transformations are illustrated in Fig. 1.

### A. Phase-space Lagrangian transformation for gyrokinetics

The particle phase-space Lagrangian is

$$\gamma = \left( \frac{e}{c} \mathbf{A} + m\mathbf{v} \right) \cdot d\mathbf{x} - \left( \frac{1}{2}mv^2 + \epsilon_\phi e\delta\phi \right) dt, \quad (1)$$

where  $\epsilon_\phi \sim e\delta\phi/T$  is the small parameter designating a small relative amplitude of fluctuations. One can first perform a gc phase-space transformation which removes the gyroangle dependence in the background magnetic field to obtain the unperturbed gc phase-space Lagrangian,<sup>2-4</sup>

$$\Gamma_{gc} \equiv \left( \frac{e}{c} \mathbf{A} + p_{\parallel gc} \mathbf{b} \right) \cdot d\mathbf{R}_{gc} + \frac{\mu_{gc} B}{\Omega} d\Theta - \left( \mu_{gc} B + \frac{p_{\parallel gc}^2}{2m} \right) dt. \quad (2)$$

Here,  $(\mathbf{R}_{gc}, p_{\parallel gc}, \mu_{gc}, \Theta)$  are gc phase-space coordinates:  $\mathbf{R}_{gc}$  denotes the gc position,  $p_{\parallel gc}$  is the kinetic parallel gc momentum,  $\mu_{gc}$  is the gc magnetic moment, and  $\Theta$  is the gc gyroangle. Catto presented a useful preliminary transformation from particle to gc variables which was first used for linear gyrokinetic theory, but remains to be useful for nonlinear derivation as well.<sup>39</sup>

Next, the gy phase-space transformation is needed to remove the gyroangle dependence introduced by the fluctuation  $\delta\phi(\mathbf{R}_{gc} + \boldsymbol{\rho}, t) = \delta\phi_{gc}(\mathbf{R}_{gc}, p_{\parallel gc}, \mu_{gc}, \Theta, t)$ . A standard derivation leads to the gy phase-space Lagrangian<sup>5,6,8,11</sup> given by

$$\Gamma_{gy} = \left( \frac{e}{c} \mathbf{A} + p_{\parallel gy} \mathbf{b} \right) \cdot d\mathbf{R}_{gy} - \left( \mu_{gy} B + \frac{p_{\parallel gy}^2}{2m} + \epsilon_\phi e \delta\Psi_{gy} \right) dt, \quad (3)$$

where the effective gyrocenter perturbed potential is

$$\delta\Psi_{gy} \equiv \langle \delta\phi_{gc} \rangle - \epsilon_\phi \frac{e}{2B} \frac{\partial}{\partial\mu} \langle \delta\tilde{\phi}_{gc}^2 \rangle \quad (4)$$

with  $\delta\tilde{\phi}_{gc} \equiv \delta\phi_{gc} - \langle\delta\phi_{gc}\rangle$ , the bracket  $\langle\cdots\rangle$  denotes a gyrophase average, and the term  $\sim c/(B\Omega)\langle\nabla\int d\bar{\theta}\delta\tilde{\phi}_{gc}\times\mathbf{b}\cdot\nabla\delta\tilde{\phi}_{gc}\rangle$  is ignored.<sup>14</sup> Here, we keep the second order of the effective potential, and the FLR effects remain intact. For simplicity, “gy” is omitted in the following. The classical polarization<sup>10,14</sup> originates from the pull-back transformation from gy to gc, and then to particle, phase space.

## B. Phase-space Lagrangian transformation for bounce-kinetics

Most of the existing bounce-kinetic theories<sup>18,19</sup> and neoclassical polarization theories<sup>18,27</sup> have ignored the FLR effects which are smaller than the FBW effects in the long wavelength regime. However, in the short wavelength regime, it’s premature to assume that apriori. We start from the gy phase-space Lagrangian which already includes the FLR effects, and apply one more two-step transformation scheme to obtain the FBW effects.

Following a procedure similar to that in gyrokinetics, we perform the bgc transformation which eliminates the bounce-angle dependence in the lowest-order (equilibrium) gy phase-space Lagrangian. Then, we remove the bounce-angle dependence in the perturbed part of the bgc phase-space Lagrangian which includes the FLR effects to obtain the bounce-angle independent bgy phase-space Lagrangian. We note that the bounce angle here refers to the bounce phase of trapped particles as well as the transit phase of passing particles. By starting from the gy phase-space Lagrangian, we can decouple the neoclassical polarization from the classical part. We can also obtain the neoclassical polarization including not only the FBW but also the FLR effects, for arbitrary radial wavelength, by keeping the FLR effects in the perturbed parts of the Lagrangian. We will present this in Sec. III.

At first, we consider the lowest-order gy phase-space Lagrangian in the  $\epsilon_\phi$  ordering, i.e., in the absence of the perturbed potential in Eq. (3),

$$\Gamma_{gy0} = \left(\frac{e}{c}\mathbf{A} + p_{\parallel}\mathbf{b}\right) \cdot d\mathbf{R} - \left(\mu B + \frac{p_{\parallel}^2}{2m}\right) dt. \quad (5)$$

Here, we drop the term  $\frac{\mu B}{\Omega}d\Theta$ , because we are not interested in the bounce-averaged gyrophase motion,<sup>17,18</sup> and the gy position  $\mathbf{R}$  can be denoted by the magnetic coordinates  $(\alpha, \beta, s)$ .  $\alpha \equiv \varphi - q\theta$  is along the binormal (nonradial perpendicular) direction, where  $\varphi$  and  $\theta$  are the toroidal and poloidal angles, respectively, and  $q$  is the safety factor;  $\beta \equiv \psi(r)$

is the poloidal flux and is along the radial direction;  $s \equiv qR_0\theta$  denotes the distance along the magnetic field line, where  $R_0$  is the major radius. Then, the magnetic field  $\mathbf{B}$  can be written as  $\nabla\alpha \times \nabla\beta$  by choosing a gauge  $\mathbf{A} = \alpha\nabla\beta$ . In the magnetic coordinates,  $\Gamma_{gy0}$  becomes<sup>18,19</sup>

$$\Gamma_{gy0} = \frac{e}{c}y^2dy^1 + p_{\parallel}\mathcal{R}_a dy^a + p_{\parallel}ds - \left( \mu B(\mathbf{y}, s) + \frac{p_{\parallel}^2}{2m} \right) dt, \quad (6)$$

where  $(y^1, y^2) = (\beta, \alpha)$  and  $\mathcal{R}_a = \mathbf{b} \cdot (\partial\mathbf{R}/\partial y^a)$ . The bounce (transit) motion takes place in the  $(p_{\parallel}, s)$  plane which can be canonically transformed to action-angle coordinates. The parallel momentum  $p_{\parallel} = mv_{\parallel}$  can be written as  $\sigma\sqrt{2m(E - \mu B_0(\mathbf{y}, s))} \simeq 2\sigma\sqrt{\epsilon m E} \sqrt{\kappa^2 - \sin^2 \frac{\theta}{2}}$ , where  $\sigma = \pm 1$  labels the sign of  $v_{\parallel}$ ,  $E \equiv \mu B(s_0) \equiv \mu B(s_1)$  defines the turning points, and  $\kappa$  is the pitch angle, with trapped particles corresponding to  $0 \leq \kappa < 1$  and passing particles corresponding to  $1 < \kappa \leq \sqrt{\frac{1+\epsilon}{2\epsilon}}$ .

Considering a high aspect ratio, concentric circular equilibrium, for lowest-order bounce (transit) motion, the bounce (transit) action  $J_{b(t)}$ <sup>17-19</sup> is given by

$$\begin{aligned} J_{b(t)} &= \begin{cases} \frac{1}{\pi} \int_{-\theta_t}^{\theta_t} d\theta \, 2qR_0\sqrt{\epsilon m E} \sqrt{\kappa^2 - \sin^2 \frac{\theta}{2}} & \text{for trapped particles} \\ \frac{1}{2\pi} \int_{-\pi}^{\pi} d\theta \, 2qR_0\sqrt{\epsilon m E} \sqrt{\kappa^2 - \sin^2 \frac{\theta}{2}} & \text{for passing particles} \end{cases} \\ &= \begin{cases} \frac{8}{\pi} qR_0\sqrt{\epsilon m E} [E(\kappa) + (\kappa^2 - 1)K(\kappa)] \\ \frac{4}{\pi} qR_0\sqrt{\epsilon m E} \kappa E(\kappa^{-1}), \end{cases} \end{aligned} \quad (7)$$

the bounce (transit) frequency  $\omega_{b(t)}$  is defined as

$$\begin{aligned} \omega_{b(t)} &= \begin{cases} \pi \left( \int_{-\theta_t}^{\theta_t} \frac{qR_0 d\theta}{2\sqrt{\epsilon E/m} \sqrt{\kappa^2 - \sin^2 \frac{\theta}{2}}} \right)^{-1} & \text{for trapped particles} \\ 2\pi \left( \int_{-\pi}^{\pi} \frac{qR_0 d\theta}{2\sqrt{\epsilon E/m} \sqrt{\kappa^2 - \sin^2 \frac{\theta}{2}}} \right)^{-1} & \text{for passing particles} \end{cases} \\ &= \begin{cases} \frac{1}{qR_0} \sqrt{\frac{\epsilon E}{m}} \frac{\pi}{2K(\kappa)} \\ \frac{1}{qR_0} \sqrt{\frac{\epsilon E}{m}} \frac{\pi \kappa}{K(\kappa^{-1})}, \end{cases} \end{aligned} \quad (8)$$

where  $K(\kappa)$  and  $E(\kappa)$  are complete elliptic integrals of the first and second kinds, and the

bounce (transit) angle  $\xi_{b(t)}$  has the following expressions:

$$\xi_{b(t)} = \begin{cases} \pi + \sigma\omega_b \int_{-\theta_t}^{\theta} \frac{qR_0 d\theta'}{2\sqrt{\epsilon E/m} \sqrt{\kappa^2 - \sin^2 \frac{\theta'}{2}}} & \text{for trapped particles} \\ \pi + \sigma\omega_t \int_{-\pi}^{\theta} \frac{qR_0 d\theta'}{2\sqrt{\epsilon E/m} \sqrt{\kappa^2 - \sin^2 \frac{\theta'}{2}}} & \text{for passing particles} \end{cases}. \quad (9)$$

This lowest-order bounce (transit) motion in the  $(s, p_{\parallel})$  phase plane is shown in Fig. 3.

In the following, we ignore the indices of the action angle variables for simplicity, but we should note that  $J_b, \xi_b$  are used for trapped particles, and  $J_t, \xi_t$  for passing particles. The space coordinate along the field line  $s$  is dependent on the action-angle coordinates. Therefore the lowest-order gyrocenter phase-space Lagrangian, Eq. (6), is also bounce-angle dependent. The Lie perturbed transformation can be applied to remove the bounce-angle dependence and to obtain the bgc phase-space Lagrangian:

$$\bar{\Gamma}_0 = \frac{e}{c} \bar{y}^2 d\bar{y}^1 + \bar{J} d\bar{\xi} - H_0(\bar{\mathbf{y}}, \bar{J}) dt, \quad (10)$$

where

$$\begin{aligned} \bar{y}^a &= y^a + g_1^a, \\ \bar{J} &= J + g_1^J, \\ \bar{\xi} &= \xi + g_1^{\xi}, \end{aligned} \quad (11)$$

with

$$g_1^a = \eta^{ab} \frac{c}{e} \left[ \frac{p_{\parallel}}{m} \mathcal{R}_b - \frac{\partial}{\partial y^b} \int_0^J dJ' \left( \frac{p_{\parallel}}{m} \frac{\partial s}{\partial J'} \right) \right], \quad (12)$$

and  $\eta^{11} = \eta^{22} = 0, \eta^{12} = -\eta^{21} = -1$ . In the present paper, “-” denotes a bgc phase space physical quantity.  $\bar{y}^a$  is the bgc position which denotes both the banana center position for trapped particles and the transit center position (located at the outboard midplane on the transit-averaged reference flux surface, a transit equivalent of the banana center) for passing particles.  $g_1^J$  and  $g_1^{\xi}$  are not needed for our purpose of deriving the polarization density, so we omit them.

Next, the bgy phase space transformation is needed, because the perturbed bgc phase-space Lagrangian

$$\bar{\Gamma}_1 + \bar{\Gamma}_2 = - \left[ \epsilon_{\phi} e \langle \delta\phi_{gc} \rangle(\bar{\mathbf{y}}, \bar{J}, \bar{\xi}, t) - \epsilon_{\phi}^2 \frac{e}{2B} \frac{\partial}{\partial \mu} \overline{\langle \delta\tilde{\phi}_{gc}^2 \rangle}(\bar{\mathbf{y}}, \bar{J}, \bar{\xi}, t) \right] dt, \quad (13)$$

is also bounce-angle dependent. Note that it includes the FLR effects, which is different from the previous works,<sup>18,19</sup> see Fig. 1. This enable us to obtain the neoclassical polarization affected by the FLR effects, which will be presented in the next section. In order to obtain a total bounce-angle independent Lagrangian, the bounce-angle averaging defined by

$$\langle A \rangle_{b(t)} = \frac{1}{2\pi} \oint d\bar{\xi} A = \begin{cases} \frac{1}{2\pi} \int_{-\theta_t}^{\theta_t} d\theta q R_0 \frac{\omega_b}{|v_{\parallel}|} \sum_{\sigma} A & \text{for trapped particles} \\ \frac{1}{2\pi} \int_{-\pi}^{\pi} d\theta q R_0 \frac{\omega_t}{|v_{\parallel}|} A & \text{for passing particles} \end{cases} \quad (14)$$

is introduced. After the Lie perturbed transformation from bgc phase space to bgy phase space, we have

$$\hat{\Gamma} = \frac{e}{c} \hat{y}^2 d\hat{y}^1 + \hat{J} d\hat{\xi} - \left[ H_0(\hat{\mathbf{y}}, \hat{J}) + \epsilon_{\phi} e \delta \Psi_{bgy} \right] dt, \quad (15)$$

$$\delta \Psi_{bgy} = \langle \overline{\langle \delta \phi_{gc} \rangle} \rangle_{b(t)} - \epsilon_{\phi} \frac{e}{2B} \frac{\partial}{\partial \hat{\mu}} \langle \overline{\langle \delta \tilde{\phi}_{gc}^2 \rangle} \rangle_{b(t)} - \epsilon_{\phi} \frac{e}{2\omega_{b(t)}} \frac{\partial}{\partial \hat{J}} \langle \delta \tilde{\phi}_{bgc}^2 \rangle_{b(t)} \quad (16)$$

$$G_1^J = \frac{e}{\omega_{b(t)}} \delta \tilde{\phi}_{bgc}, \quad (17)$$

with  $\delta \tilde{\phi}_{bgc} = \overline{\langle \delta \phi_{gc} \rangle} - \langle \overline{\langle \delta \phi_{gc} \rangle} \rangle_{b(t)}$ . The term  $\sim \frac{c}{2} \eta^{ab} \left\langle \frac{\partial}{\partial \hat{y}^b} \left( \frac{1}{\omega_{b(t)}} \int^{\hat{\xi}} \delta \tilde{\phi}_{bgc} d\hat{\xi}' \right) \frac{\partial}{\partial \hat{y}^a} \delta \tilde{\phi}_{bgc} \right\rangle_{b(t)}$  is ignored, which is similar to the case in gyrokinetics.<sup>14</sup> The second and the last terms in the effective bgy potential Eq. (16) are corresponding to the classical and the neoclassical polarization, respectively, where the second term was not contained in Ref. 18. We note that Eq. (16) is the electrostatic limit of Eq. (44) in Ref. 19, but we keep the FLR effects which were ignored in that work. “ $\sim$ ” in this paper means a physical quantity in bgy phase space. It can be shown that the  $G_1^J$  component of the generator of this transformation contributes dominantly to the polarization density. Therefore, we neglect the other components of the generator. This is very similar to the case in gyrokinetics<sup>14</sup>.

### III. DERIVATION OF GENERAL POLARIZATION

In the last section, we presented the principal results of the transformation from particle to gy phase space for gyrokinetics, and those from gy to bgy phase space for bounce kinetics. Fong and Hahm showed that the neoclassical polarization density can be derived via modern bounce-kinetics, although only trapped particles were included.<sup>18</sup> The classical polarization density was not presented in Ref. 18, and their bgy Hamiltonian did not contain the second

order ponderomotive potential associated with the classical polarization. Brizard presented the bgy Hamiltonian including both the second order ponderomotive potential for full electromagnetic field fluctuations, but he did not consider the FLR effects.<sup>19</sup> While the classical and neoclassical polarization were not explicitly discussed in Ref. 19, the ponderomotive potential has one to one correspondence with the associated polarization density as discussed more recently.<sup>13</sup> As emphasized in Ref. 5 and in Ref. 13, the ponderomotive potential is necessary for the energy conservation when the polarization density is kept in the gyrokinetic poisson's equation. The polarization density can be derived from functional derivative of the effective potential.<sup>13</sup> In this sense, one could include the linear potential's contribution when one defines the polarization density.<sup>13</sup> However, we choose to define the polarization density in the usual way (including only the ponderomotive potential's contribution) which makes the comparisons to the previous numerical results<sup>37,38</sup> more transparent. For instance, in Eq. (54) of Ref. 40, only the last term corresponds to polarization density according to our definition, while the last two terms represent polarization density according to the definition in Ref. 13. Of course, there's no contradiction since we include the linear potential related polarization density in the definition of bounce-averaged bgy density.

Now we express the real particle density in terms of the distribution function in the gy phase space, and eventually in the bgy phase space. It consists of two consecutive pull-back transformations which are from gy to particle phase space, and then from bgy to gy phase space, respectively. The first one recovers the classical polarization density, while the second one yields the neoclassical polarization density. These pull-back transformations are illustrated in Fig. 2.

For the first pull-back transformation, following the steps in Refs. 5 and 8, the real particle density can be written in terms of the distribution function in the gy phase space,

$$\begin{aligned} n(\mathbf{x}, t) &= \int d^6 Z (T_{gy}^* F_{gy})(Z) \delta^3(T_{gc}^{-1} \mathbf{R} - \mathbf{x}) \\ &= \int d^6 Z \left[ F_{gy}(Z) + \left( G_1^\mu \frac{\partial}{\partial \mu} + G_1^{\mathbf{R}} \cdot \nabla + G_1^{p\parallel} \frac{\partial}{\partial p\parallel} \right) F_{gy}(Z) \right] \delta^3(T_{gc}^{-1} \mathbf{R} - \mathbf{x}) \end{aligned} \quad (18)$$

where the first term is the gyroaveraged gy density (denoted by  $N_{gy}$ ), the last three terms on the R.H.S contribute to the classical polarization, i.e., the difference between the real particle density and the gyroaveraged gy density. It can be shown that, compared to the  $G_1^\mu$  term, the  $G_1^{\mathbf{R}}$  and  $G_1^{p\parallel}$  terms are of higher order. Therefore, these can be ignored.<sup>14</sup> Then,

the real particle density is

$$n(\mathbf{x}, t) = N_{gy}(\mathbf{x}, t) + n_{cl}(\mathbf{x}, t), \quad (19)$$

with

$$N_{gy}(\mathbf{x}, t) = \int d^6 Z F_{gy}(Z) \delta^3(T_{gc}^{-1} \mathbf{R} - \mathbf{x}), \quad (20)$$

$$n_{cl}(\mathbf{x}, t) = \int d^6 Z G_1^\mu \frac{\partial}{\partial \mu} F_{gy}(Z) \delta^3(T_{gc}^{-1} \mathbf{R} - \mathbf{x}). \quad (21)$$

The second pull-back transformation from bgy to gy phase space is similar to the first one. The transformation from gy coordinates  $Z$  to bgc coordinates  $\bar{Z} \equiv T_{bgc} Z$  enables us to express the gyroaveraged gy density in Eq. (20) by integration over bgc phase space, i.e.,

$$N_{gy}(\mathbf{x}, t) = \int d^6 \bar{Z} \bar{F}(\bar{Z}) \delta^3(T_{gc}^{-1} T_{bgc}^{-1} \bar{\mathbf{R}} - \mathbf{x}). \quad (22)$$

Here, the identity  $F_{gy}(Z) \equiv \bar{F}(\bar{Z})$  has been used, with  $d^6 \bar{Z} \equiv \frac{B}{m^2} ||\partial Z / \partial \bar{Z}|| d\bar{\mathbf{y}} d\bar{J} d\bar{\xi} d\bar{\mu} d\bar{\Theta}$ .  $\bar{Z}$  is a dummy variable. It can therefore be replaced by the bgy coordinate  $\hat{Z} \equiv T_{bgy} \bar{Z}$ . The bgc distribution function can be obtained by a pull-back transformation of the bgy distribution function,

$$\bar{F}(\bar{Z}) \equiv (T_{bgy}^* \hat{F})(\bar{Z}). \quad (23)$$

By combining the relationship between  $\bar{F}$  and  $\hat{F}$  given above and replacing the dummy variable  $\bar{Z}$  by  $\hat{Z}$ , the integral expression in Eq. (22) can be written as

$$\begin{aligned} N_{gy}(\mathbf{x}, t) &= \int d^6 \hat{Z} (T_{bgy}^* \hat{F})(\hat{Z}) \delta^3(T_{gc}^{-1} T_{bgc}^{-1} \hat{\mathbf{R}} - \mathbf{x}) \\ &= \int d^6 \hat{Z} \left[ \hat{F}(\hat{Z}) + \left( G_1^J \frac{\partial}{\partial J} + G_1^a \frac{\partial}{\partial \hat{y}^a} \right) \hat{F}(\hat{Z}) \right] \delta^3(T_{gc}^{-1} T_{bgc}^{-1} \hat{\mathbf{R}} - \mathbf{x}), \end{aligned} \quad (24)$$

where the first term  $\hat{N}(\mathbf{x}, t) = \int d^6 \hat{Z} \hat{F}(\hat{Z}) \delta^3(T_{gc}^{-1} T_{bgc}^{-1} \hat{\mathbf{R}} - \mathbf{x})$  is the bounce-averaged bgy density, the last two terms contribute to the difference between the gyroaveraged gy density and the bounce-averaged bgy density, which is the well known neoclassical polarization density. It's noted that we can also show that the  $G_1^a$  term is much smaller than the  $G_1^J$  term, so we just keep the  $G_1^J$  term in the neoclassical polarization density, i.e.,

$$n_{nc}(\mathbf{x}, t) = \int d^6 \hat{Z} G_1^J \frac{\partial}{\partial J} \hat{F}(\hat{Z}) \delta^3(T_{gc}^{-1} T_{bgc}^{-1} \hat{\mathbf{R}} - \mathbf{x}). \quad (25)$$

Finally, the real particle density is given by

$$n(\mathbf{x}, t) = \hat{N}(\mathbf{x}, t) + n_{cl}(\mathbf{x}, t) + n_{nc}(\mathbf{x}, t). \quad (26)$$

We have systematically derived the general polarization density which is the difference between the real particle density and the bounce-averaged bgy density. This, of course, consists of two parts, i.e., the classical and neoclassical polarization densities. The classical part comes from the difference between the real particle and the gyroaveraged gy densities, and the neoclassical part comes from the difference between the gyroaveraged gy and the bounce-averaged bgy densities. Another point is that the  $G_1^J$  in the neoclassical polarization density Eq. (25) retains not only the FBW but also the FLR effects, which can be seen from Eq. (17) in the last section. It ensures the energy conserving of the bounce-kinetic system.

#### IV. CALCULATION OF GENERAL POLARIZATION FOR ARBITRARY GYRORADIUS AND POLOIDAL GYRORADIUS

The well known limiting form of the classical polarization density, for  $F_{gy}$  which is Maxwellian in  $\mu$ , is

$$n_{cl}(\mathbf{x}, t) \simeq \sum_k \left(-\frac{e}{T}\right) N \delta\phi_k e^{iS(\mathbf{x}_\perp)} (1 - \Gamma_0(b)), \quad (27)$$

where  $N = \int d^6 Z F(Z) \delta^3(\mathbf{R} - \mathbf{x})$  is the gy density, and  $\Gamma_n(b) = I_n(b) e^{-b}$ , and  $I_n$  is the modified Bessel function of order  $n$ , where  $b = k_\perp^2 T / (m\Omega^2)$  and the wave vector is defined by  $\mathbf{k}_\perp = \nabla S$ .

Now, we evaluate the neoclassical polarization density. Recognizing that the neoclassical polarization plays an important role in the zonal flow related physics,<sup>41</sup> we consider only an axisymmetric fluctuation,<sup>27</sup> i.e.,

$$\langle \delta\phi_{gc} \rangle = \sum_k J_0(k_r \rho) \delta\phi_k e^{iS(\psi)}, \quad (28)$$

where  $J_0(k_r \rho)$  is the zeroth-order Bessel function, and  $\rho = v_\perp / \Omega$  is the gyroradius. We keep the FLR effects which were ignored in Refs. 18-19.

### A. Contribution from Trapped Particles

First, we calculate the trapped particles' contribution to the neoclassical polarization. For trapped particles, the bounce angle in Eq. (9) is given by

$$\kappa \cos \xi \simeq \sin \frac{\theta}{2}. \quad (29)$$

The bounce deviation in the radial direction during bounce motion from Eq. (12) written in terms of action-angle coordinates is

$$g_1^1 \simeq 2 \frac{mc}{e} R_0 \sqrt{\epsilon E/m} \kappa \sin \xi. \quad (30)$$

It follows that the bounce-averaged fluctuation in Eq. (14) can be given by

$$\begin{aligned} \langle \overline{\langle \delta \phi_{gc} \rangle} \rangle_b &= \sum_k J_0(k_r \hat{\rho}) \delta \phi_k e^{iS(\hat{\psi})} \langle e^{-i2\sqrt{\epsilon} k_r \rho_{\theta T} \sqrt{E/T} \kappa \sin \xi} \rangle_b \\ &= \sum_k J_0(k_r \hat{\rho}) J_0(a\kappa) \delta \phi_k e^{iS(\hat{\psi})}, \end{aligned} \quad (31)$$

where  $a = 2\sqrt{\epsilon} k_r \rho_{\theta T} \sqrt{E/T}$ ,  $\rho_{\theta T} = (T/m)^{1/2}/\Omega_p$  is the thermal poloidal gyroradius,  $\Omega_p = eB_\theta/(mc)$  is the poloidal gyrofrequency, and  $J_0(a\kappa)$  represents the FBW effects.

Following the procedure in Ref. 18, the neoclassical polarization density for trapped particles is

$$\begin{aligned} n_{nc}^{tr}(r, \theta, t) &= \int' \frac{B\omega_b}{m^2 |v_{||}|} d\hat{y}^1 d\hat{y}^2 d\hat{J} d\hat{\xi} d\hat{\mu} d\hat{\Theta} \delta(\hat{y}^a - g_1^a - x^a) \\ &\quad \times \delta\left(\hat{\xi} - g_1^\xi - h(s, \hat{J})\right) e^{-i\mathbf{k}_\perp \cdot \hat{\rho}} \frac{e}{\omega_b} \left( \langle \delta \phi_{gc} \rangle - \langle \overline{\langle \delta \phi_{gc} \rangle} \rangle_b \right) \frac{\partial \hat{F}}{\partial \hat{J}} \end{aligned} \quad (32)$$

where the prime indicates integration over trapped particles only,  $h$  denotes the relationship between  $\hat{\xi}$  and  $(s, \hat{J})$ , and the bgy distribution function is assumed to be Maxwellian,

$$\hat{F}(\hat{\mathbf{y}}, \hat{J}, \hat{\mu}, t) = \hat{N} \left( \frac{m}{2\pi T} \right)^{3/2} e^{-E/T}, \quad (33)$$

where,  $\hat{N}$  is the bgy position density. The bounce-kinetics and gyrokinetics share many common properties, but are different in the following important aspects. The bounce angle  $\hat{\xi}$  directly depends on the field line, whereas the gyroangle does not.<sup>18</sup> Furthermore, the bounce radius depends on the bounce angle, but gyroradius is independent of gyroangle. The neoclassical polarization density is explicitly dependent on field line.<sup>18</sup> The flux-surface

averaged part of the neoclassical polarization density is a quantity of primary importance for application to zonal flow related problems, so we introduce flux surface averaging  $\langle \dots \rangle_{flux} = (2\pi)^{-1} \int_{-\pi}^{\pi} d\theta (\dots)$ . After flux-surface averaging and integrating over gyroangle, bounce angle and bgy position, Eq. (32) becomes

$$\begin{aligned} \langle n_{nc}^{tr} \rangle_{flux}(r, t) &\simeq \sum_k \left(-\frac{e}{T}\right) \delta\phi_k e^{iS(r)} \hat{N} \left(\frac{2}{\pi}\right)^{3/2} \sqrt{\epsilon} \int_0^\infty dt^2 t e^{-t^2} J_0^2(\sqrt{2}k_r \rho_T t) \frac{1}{2\pi} \int_{-\pi}^{\pi} d\theta \\ &\times \int_{\kappa_0}^1 d\kappa^2 q R_0 K(\kappa) \frac{\omega_b}{|v_{\parallel}|} \left[ 1 - \langle e^{-ia\kappa \sin \hat{\xi}} \rangle_b \left( e^{ia\sqrt{\kappa^2 - \sin^2 \frac{\theta}{2}}} + \text{c.c.} \right) \right] \end{aligned} \quad (34)$$

where  $\rho_T$  is the thermal gyroradius,  $t = \sqrt{E/T}$ , and  $\kappa_0 = \sin(\theta/2)$ . The first term in the bracket of last equation come from the the bounce angle integration from 0 to  $\pi$  ( $\sigma = -$ ), and the conjugated term from  $\pi$  to  $2\pi$  ( $\sigma = +$ ). By exchanging the order of the  $\theta$  and  $\kappa^2$  integration

$$\int_{-\pi}^{\pi} d\theta \int_{\kappa_0}^1 d\kappa^2 = \int_0^1 d\kappa^2 \int_{-\theta_t}^{\theta_t} d\theta,$$

we have

$$\begin{aligned} \langle n_{nc}^{tr} \rangle_{flux}(r, t) &= \sum_k \left(-\frac{e}{T}\right) \delta\phi_k e^{iS(r)} \hat{N} \left(\frac{2}{\pi}\right)^{3/2} \sqrt{\epsilon} \int_0^\infty dt^2 t e^{-t^2} J_0^2(\sqrt{2}k_r \rho_T t) \\ &\times \int_0^1 d\kappa^2 K(\kappa) \left( 1 - |\langle e^{-ia\kappa \sin \hat{\xi}} \rangle_b|^2 \right), \end{aligned} \quad (35)$$

where the bounce average for trapped particles in Eq. (14) has been used. The flux-surface-averaged neoclassical polarization density quantifies the shielding effects with respect to the flux surface, but not around the center point (the bounce center for trapped particles and the transit center for passing particles). Now we define the neoclassical susceptibility  $\chi_{k,nc}^{tr}$  in Fourier space,

$$\langle n_{nc}^{tr} \rangle_{flux} / \hat{N} = \sum_k \left(-\frac{e}{T}\right) \delta\phi_k e^{iS(r)} \chi_{k,nc}^{tr}. \quad (36)$$

Here, the neoclassical susceptibility  $\chi_{k,nc}^{tr}$  can be written as

$$\chi_{k,nc}^{tr} = \left(\frac{2}{\pi}\right)^{3/2} \sqrt{\epsilon} \int_0^\infty dt^2 t e^{-t^2} J_0^2(\sqrt{2}k_r \rho_T t) \int_0^1 d\kappa^2 K(\kappa) [1 - J_0^2(a\kappa)], \quad (37)$$

after using Eq. (31).

Next, we consider limiting cases. For the short wavelength limit (high  $k_r$ ), i.e.,  $k_r \rho_{\theta T} > k_r \rho_T \gg 1$ , we can use the large argument asymptotic form of the Bessel functions in Eq. (37),

for large gyroradius and large poloidal gyroradius limit, i.e.,  $J_0(z) \simeq \sqrt{2/(\pi z)} \cos(z - \pi/4)$ . After integration, we can get

$$\chi_{k,nc}^{tr,short} = \frac{4\sqrt{\epsilon}}{\pi^2\sqrt{\pi}} \frac{1}{k_r\rho_T} [1 - \Gamma_{tr}(\sqrt{\epsilon}k_r\rho_{\theta T})], \quad (38)$$

with

$$\Gamma_{tr}(\sqrt{\epsilon}k_r\rho_{\theta T}) = \frac{\text{Catalan}}{\sqrt{\pi\epsilon}k_r\rho_{\theta T}},$$

and Catalan  $\simeq 0.915966$  is a constant.

For the intermediate wavelength limit, i.e.,  $k_r\rho_T \ll 1$  and  $k_r\rho_{\theta T} \gg 1$ , the FLR effects can be neglected, i.e.,  $J_0(\sqrt{2}k_r\rho_T t) \simeq 1$ . The FBW effects  $J_0(a\kappa)$ , on the other hand, can still be asymptotically expanded in the large argument limit. After integration, we can get

$$\chi_{k,nc}^{tr,m} = \frac{\sqrt{8\epsilon}}{\pi} [1 - \Gamma'_{tr}(\sqrt{\epsilon}k_r\rho_{\theta T})], \quad (39)$$

with  $\Gamma'_{tr} = 2\Gamma_{tr}/\pi$ .

For the long wavelength limit (low  $k_r$ ), i.e.,  $k_r\rho_T < k_r\rho_{\theta T} \ll 1$ , the FLR effect can also be neglected. The lowest-order FBW effects can be obtained by expanding the Bessel function in powers of small poloidal gyroradius, i.e.,  $J_0(a\kappa) \simeq 1 - a^2\kappa^2/4$ . Then we can get the neoclassical susceptibility for trapped particles in the small gyroradius and the small but finite poloidal gyroradius (FPG) limit,

$$\chi_{k,nc}^{tr,long} \simeq 1.5\epsilon^{3/2}k_r^2\rho_{\theta T}^2. \quad (40)$$

## B. Contribution from Passing Particles

The procedure is similar to that for trapped particles. The transit angle for passing particles in Eq. (9) is given by

$$\xi \simeq \sigma\theta. \quad (41)$$

The transit deviation in the radial direction during the oscillatory motion written in terms of action-angle coordinates is

$$g_1^1 \simeq -2\sigma \frac{mc}{e} R_0 \sqrt{\epsilon E/m} \sqrt{\kappa^2 - \sin^2 \frac{\xi}{2}}. \quad (42)$$

Given the results above, the transit-averaged fluctuation can be written as

$$\langle \overline{\delta\phi_{gc}} \rangle_t = \sum_k J_0(k_r \hat{\rho}) \delta\phi_k e^{iS(\hat{\psi})} \left\langle e^{i\sigma a \sqrt{\kappa^2 - \sin^2(\hat{\xi}/2)} \right\rangle_t. \quad (43)$$

The difference between the bounce average for trapped particles and the transit average for passing particles is apparent in the relationship between the field line variable and the angle variable shown in Eq. (29) and Eq. (41). Similar to the trapped particle part, using the transit action  $\hat{J}_t$  in Eq. (7) and the transit average in Eq. (14) and (43), the neoclassical susceptibility for passing particles is given by

$$\chi_{k,nc}^p \simeq \left(\frac{2}{\pi}\right)^{3/2} \sqrt{\epsilon} \int_0^\infty dt^2 t e^{-t^2} J_0^2(\sqrt{2} k_r \rho_T t) \int_1^{\sqrt{\frac{1+\epsilon}{2\epsilon}}} d\kappa K(\kappa^{-1}) \sum_{\sigma=\pm} \left(1 - \left| \left\langle e^{i\sigma a \sqrt{\kappa^2 - \sin^2(\hat{\xi}/2)} \right\rangle_t \right|^2\right). \quad (44)$$

Here, the transit angle integration is from  $\pi$  to  $3\pi$  ( $\sigma = +$ ) and  $-\pi$  to  $\pi$  ( $\sigma = -$ ) to include all the passing particles moving in both directions for  $p_{\parallel}$ . This is also different from trapped particles.

Next, we consider a limiting case. For the short wavelength limit (high  $k_r$ ), i.e.,  $k_r \rho_{\theta T} > k_r \rho_T \gg 1$ , we use the large argument asymptotic form of the Bessel function in Eq. (44) as in the trapped particle part. We can use the stationary phase approximation for transit averaging in the large poloidal gyroradius limit,

$$\left\langle e^{i\sigma a \sqrt{\kappa^2 - \sin^2(\hat{\xi}/2)} \right\rangle_t \simeq \sqrt{\frac{2\kappa}{\pi a}} e^{i\sigma(a\kappa - \frac{\pi}{4})}. \quad (45)$$

By using the results given above and integrating Eq. (44), we obtain

$$\chi_{k,nc}^{p,short} = \frac{\sqrt{2}}{\pi \sqrt{\pi}} \frac{1}{k_r \rho_T} \left(1 - \frac{\sqrt{8\epsilon}}{\pi}\right) (1 - \Gamma_p(\epsilon k_r \rho_{\theta T})), \quad (46)$$

with

$$\Gamma_p(\epsilon k_r \rho_{\theta T}) = \frac{1}{2\sqrt{2\pi} \epsilon k_r \rho_{\theta T}},$$

and the large aspect ratio limit, i.e.,  $\epsilon \ll 1$ , was used.  $\Gamma_p$  is inversely proportional to the strongly circulating particles' orbit  $\epsilon \rho_{\theta T}$ , which means that, for passing particles, the strongly circulating particles' contribution to the neoclassical polarization is dominant in the short wavelength limit.

For the intermediate wavelength limit, i.e.,  $k_r \rho_T \ll 1$  and  $k_r \rho_{\theta T} \gg 1$ , the FLR effects can also be neglected and the stationary phase approximation for transit averaging in the large poloidal gyroradius limit (Eq. (45)) can also be used. After integration, we can get

$$\chi_{k,nc}^{p,m} = \left(1 - \frac{\sqrt{8\epsilon}}{\pi}\right) (1 - \Gamma'_p(\epsilon k_r \rho_{\theta T})), \quad (47)$$

with  $\Gamma'_p = 2\Gamma_p/\pi$ .

For the long wavelength limit, i.e.,  $k_r \rho_T < k_r \rho_{\theta T} \ll 1$ , the FLR effects can also be neglected; the transit averaging can be obtained by expanding the exponential expression in powers of small poloidal gyroradius to the same order as for the trapped particles part,

$$\left\langle e^{i\sigma a \sqrt{\kappa^2 - \sin^2(\hat{\xi}/2)}} \right\rangle_t \simeq 1 + i\sigma a \kappa E \left(\frac{1}{\kappa}\right) \frac{2}{\pi} - \frac{1}{2} a^2 \left(\kappa^2 - \frac{1}{2}\right). \quad (48)$$

Then, we can get the neoclassical susceptibility for passing particles in the small gyroradius and small but FPG limit

$$\chi_{k,nc}^{p,long} \simeq 0.33 \epsilon^{3/2} k_r^2 \rho_{\theta T}^2. \quad (49)$$

Note that this scaling is the same as that from the trapped particles, rather than one which can be obtained from a dimensional analysis based on strongly circulating particles' orbit, i.e.,  $\chi_{k,nc}^{p,s} \approx \epsilon^2 k_r^2 \rho_{\theta T}^2$ . This implies that, for passing particles, the barely circulating particles' contribution is significant for the neoclassical polarization density in the long wavelength limit.

### C. Total Neoclassical Susceptibility

The total neoclassical susceptibility including contributions from both trapped and passing particles for the three limiting cases are

$$\chi_{k,nc} = \begin{cases} \sqrt{\frac{2}{\pi^3}} \frac{1}{k_r \rho_T} \left[ 1 - \frac{\sqrt{8\epsilon}}{\pi} \Gamma_{tr} - \left(1 - \frac{\sqrt{8\epsilon}}{\pi}\right) \Gamma_p \right] & \text{for } k_r \rho_{\theta T} > k_r \rho_T \gg 1, \\ 1 - \frac{\sqrt{8\epsilon}}{\pi} \Gamma'_{tr} - \left(1 - \frac{\sqrt{8\epsilon}}{\pi}\right) \Gamma'_p & \text{for } k_r \rho_T \ll 1 \text{ and } k_r \rho_{\theta T} \gg 1, \\ 1.83 \epsilon^{3/2} k_r^2 \rho_{\theta T}^2 & \text{for } k_r \rho_T < k_r \rho_{\theta T} \ll 1. \end{cases} \quad (50)$$

Various terms in the first line of Eq. (50) have the following physical meaning. The factor  $\sqrt{2}/(\pi\sqrt{\pi}k_r\rho_T)$  comes from the FLR effects which was kept in the perturbed gy phase-space

Lagrangian;  $\sqrt{8\epsilon}/\pi$  is the fraction of trapped particles, and  $1 - \sqrt{8\epsilon}/\pi$  is the passing particle fraction; the neoclassical polarization effects for every trapped particle and passing particle can be written as  $1 - \Gamma_{tr}(\sqrt{\epsilon}k_r\rho_{\theta T})$  and  $1 - \Gamma_p(\epsilon k_r\rho_{\theta T})$ , where  $\Gamma_{tr}$  and  $\Gamma_p$  are inversely proportional to the banana width  $\sqrt{\epsilon}\rho_{\theta T}$ , and the radial deviation from the flux surface for a strongly circulating particle  $\epsilon\rho_{\theta T}$ , respectively, in the short wavelength limit. The result in the second line is similar with that in the first line except for the absence of the FLR effects. The result in the third line for the small but FPG limiting case has the same scaling as that of Ref. 27 with a slightly different coefficient. The small difference arises since, for trapped particles, we average the fluctuation over bounce angle first, i.e., Eq. (31), and then expand the Bessel function for small argument, while in Ref. 27, they expand the exponential function in the small argument limit first, and then average over bounce angle. For passing particles, we use the approximation for the transit angle, i.e., Eq. (41), whereas the averaging in Ref. 27 has been performed directly along the field line.

We can construct a connection formula for the generalized neoclassical susceptibility for arbitrary gyroradius and poloidal gyroradius by adding the inverse of the asymptotic forms in the limiting cases in Eq. (50), and then taking the inverse of the summation,

$$\chi_{nc,k} = \left\{ \frac{1}{1.83\epsilon^{3/2}k_r^2\rho_{\theta T}^2} + \left[ 1 + \frac{\sqrt{8\epsilon}}{\pi}\Gamma'_{tr} + \left( 1 - \frac{\sqrt{8\epsilon}}{\pi} \right) \Gamma'_p \right] \frac{1}{1 + k_r^2\rho_T^2} + \sqrt{\frac{\pi^3}{2}}k_r\rho_T \left[ 1 + \frac{\sqrt{8\epsilon}}{\pi}\Gamma_{tr} + \left( 1 - \frac{\sqrt{8\epsilon}}{\pi} \right) \Gamma_p \right] \frac{k_r^2\rho_T^2}{1 + k_r^2\rho_T^2} \right\}^{-1}. \quad (51)$$

This addition of terms in the denominator may produce a smaller value of the neoclassical polarization in an intermediate region. To partially compensate this artifact, we multiply the inverse of  $\chi_{k,nc}^m$  for low  $k_r$  limit and  $\chi_{k,nc}^{short}$  for high  $k_r$  limit by the factors  $1/(1 + k_r^2\rho_T^2)$  and  $k_r^2\rho_T^2/(1 + k_r^2\rho_T^2)$ , respectively. They are slightly less than 1 in their validity regime respectively, with their sum equal to 1.

We also define the susceptibility for classical polarization. It is given by

$$\chi_{k,cl} = 1 - \langle \Gamma_0(b) \rangle_{flux}, \quad (52)$$

which is valid for arbitrary gyroradius. Finally, the general polarization including both classical and neoclassical parts for arbitrary gyroradius and poloidal gyroradius is

$$\chi_k^{total} = \chi_{k,nc} + \chi_{k,cl}, \quad (53)$$

with  $\chi_{k,nc}$  and  $\chi_{k,cl}$  given by Eqs (51) and (52) respectively.

#### D. Comparison to the previous results

We note that, in Ref. 38 the analytical results for the neoclassical polarization and residual zonal flow were extended to order of  $k_{\perp}^4 \rho_{\theta i}^4$ , where  $\rho_{\theta i}$  is ion thermal poloidal gyroradius. However, the assumption  $k_{\perp}^4 \rho_{\theta i}^4 \ll 1$  was still required. The results for arbitrary wavelength were obtained numerically. Note that the susceptibility  $\chi_k$  in our work is different from the polarization constant  $\epsilon_k^{pol}$  defined in Ref. 38 by a factor, i.e.,  $\chi_k = k_{\perp}^2 \rho_i^2 (\Omega_i^2 / \omega_{pi}^2) \epsilon_k^{pol}$ , where  $\rho_i$  is the ion thermal gyroradius,  $\Omega_i$  is the ion gyrofrequency, and  $\omega_{pi} = \sqrt{4\pi e^2 n_0 / m}$  is the ion plasma frequency.  $k_{\perp} \simeq k_r$  is used in the following. In Fig. 4, we compare our generalized neoclassical polarization, i.e., Eq. (51) with the numerical results of Ref. 38 for wavelength up to  $k_r \rho_{\theta i} = 0.7$ , inverse aspect ratio up to  $\epsilon = 0.3$ , and  $q = 1.4$ . We find very good agreement. We also compare the residual zonal flow level,  $R = \chi_{k,cl} / (\chi_{k,cl} + \chi_{k,nc})$ , between our analytical results and their numerical results for arbitrary wavelength in Fig. 5. The results in this figure is for the case that only ion polarization effect is included. From Fig. 5, we can see that our analytic results from an independent derivation using a different method agree well with theirs.

Note that our general polarization for arbitrary radial wavelength, Eq. (53) can be applied to electrons as well. In fact, when the radial wavelength decreases to be comparable to electron gyroradius  $\rho_e$ , such as for the ETG turbulence, the electron polarization effect should be also taken into account.<sup>37,38</sup> Therefore, the generalized residual zonal flow level can be written as

$$R = \frac{\tau \chi_{ik,cl} + \chi_{ek,cl}}{\tau \chi_{ik,cl} + \chi_{ek,cl} + \tau \chi_{ik,nc} + \chi_{ek,nc}}, \quad (54)$$

where  $\tau = T_e / T_i$  is the electron to ion temperature ratio.<sup>38</sup> ETG turbulence in its simplest context can be studied with adiabatic ions, i.e., with  $\chi_{ik,cl} = 1$  and  $\chi_{ik,nc} = 0$ . Then, for relatively long wavelength ETG-driven zonal flows, R-H formula for electron susceptibilities could be used for the residual zonal flow level, i.e.,

$$R = \frac{\tau + k_r^2 \rho_e^2}{\tau + k_r^2 \rho_e^2 (1 + 1.6q^2 / \sqrt{\epsilon})}. \quad (55)$$

The validity regime of this formula was discussed in Ref. 42 (Eq. (8)). They noted that the residual magnetization related to the classical polarization for ions in the  $k_{\perp} \rho_i \gg 1$  limit

can compete with the neoclassical polarization of electrons for ETG turbulence.<sup>42</sup> Fig. 6 shows that Eq. (55) (denoted by dash line) becomes a poor approximation for  $k_r \rho_e \gtrsim 0.2$  as discussed in Ref. 42. Although Xiao and Catto's analytic formula could predict the trend by keeping the next order of the FPG effects for electrons, it breaks down when  $k_r \rho_{\theta e} \gtrsim 1$ .<sup>38</sup> Until now, there has been no analytical result in that short wavelength regime. In Fig. 6, the solid line represents the residual zonal flow with our analytic connection formula Eq. (53) for electrons and adiabatic ions which behaves very well in the short wavelength regime up to  $k_r \rho_e \sim 1$ . This can be seen from Fig. 7 presented later. Also note that employing the adiabatic ion response cannot lead to a correct residual zonal flow level for long wavelength zonal flow.

Now we compare our full analytic expression Eq. (54) with the previous numerical results<sup>37,38</sup> in Fig. 7. In this figure, both ion and electron polarization effects are included. Fig. 7 shows the residual zonal flow level vs  $k_r \rho_e$  for a plasma composed of deuterium and electrons for  $\tau = 1$ ,  $q = 1.4$  and  $\epsilon = 0.2$ . The results of Ref. 38 have been converted from  $\rho_i$  to  $\rho_e$  for deuterium. It is shown that our analytic result behaves very similar to their numerical results in the whole regime of  $k_r \rho_e$ . Of course, the readers should be reminded that the residual zonal flow level  $R$  is not the only factor in determining the relative intensity of zonal flows for ETG turbulence in comparison to that for ITG turbulence as discussed in Ref. 37 and 42.

Finally, we compare with the result of Ref. 37 for the limiting case  $\epsilon = 0$ . We plot the residual zonal flow level for  $\epsilon = 0.1, 10^{-3}, 10^{-5}, 0$ , respectively in Fig. 8. We can see that our results converge in the  $\epsilon = 0$  limit with decreasing  $\epsilon$ . We note that  $\epsilon = 0$  is a rather subtle and arbitrary limit. For instance, a cylindrical limit corresponds to  $\epsilon = 0$  and  $q = 0$  with  $\epsilon/q \approx B_\theta/B_T$  fixed, rather than the limit considered here ( $\epsilon = 0$ , for fixed  $q$ ). While our analytic formulate deviates moderately from various previous numerical results in particular parameter regimes, its overall behavior recovers their trends for a wide range of parameters. Therefore, it should be useful for various analytic applications which will eventually elucidate parametric dependencies.

## V. CONCLUSIONS

In the present work, we have systematically derived a generalized expression for polarization density for arbitrary gyroradius and poloidal gyroradius using modern gyrokinetics and bounce-kinetics. For bounce-kinetics, we start from the Lagrangian in gy phase space rather than gc phase space and keep the FLR effects, which is different from previous works.<sup>18,19</sup> As a consequence, the classical and neoclassical polarization densities are naturally obtained via pull-back transformations which are based on phase-space Lagrangian Lie-transform perturbation methods. We further elucidate their physical meaning. Another important result obtained from this procedure is that not only the FBW but also the FLR effects are retained in the neoclassical polarization.

We take into account the passing particles contribution to the neoclassical polarization separately from the contribution from the trapped particles. In general, the neoclassical polarization density has an explicit dependence on the field line.<sup>18</sup> In this work, we have obtained the flux-surface averaged neoclassical polarization which quantifies the shielding effects with respect to the flux surface, rather than around the orbit center point. By connecting the results for asymptotic limits in both small and large orbit widths, we get the generalized neoclassical polarization for arbitrary gyroradius and poloidal gyroradius. Finally, by adding the classical polarization for arbitrary gyroradius, we obtain an analytical formula for the general polarization. We find that our analytical results compare very well with the numerical results in Ref. 37-38 for the case including only ion dynamics as well as for the ETG turbulence including both ion and electron polarization effects.

The formalism presented in this paper can be applied for variety of microturbulence theories including the trapped particle mode turbulence and collisionless damping of zonal flows. These include study of a nonlinear interaction between microturbulence at disparate scales, and of the short spatial scale zonal flow generation which has been observed in simulation of TEM turbulence.<sup>45,46</sup>

### Acknowledgments

We thank A. Brizard, Y. Xiao, F. L. Hinton, G. W. Hammett, L. Chen, G. Rewoldt, and G. Dif-Pradalier for useful comments on our work. This work was supported by the China

Scholarship Council (LW), the U. S. Department of Energy Contract No. DE-AC02-76-CHO-3073 (TSH, LW), the U. S. DOE SciDAC center for Gyrokinetic Particle Simulation of Turbulent Transport in Burning Plasmas and the U. S. DOE SciDAC-FSP Center for Plasma Edge Simulation (TSH).

- 
- <sup>1</sup> E. A. Frieman and L. Chen, *Phys. Fluids* **25**, 502 (1982).
- <sup>2</sup> R. G. Littlejohn, *Phys. Fluids* **24**, 1730 (1981).
- <sup>3</sup> R. G. Littlejohn, *J. Math. Phys.* **23**, 742 (1982).
- <sup>4</sup> R. G. Littlejohn, *J. Plasma Phys.* **29**, 111 (1983).
- <sup>5</sup> D. H. E. Dubin, J. A. Krommes, C. Oberman, and W. W. Lee, *Phys. Fluids* **26**, 3524 (1983).
- <sup>6</sup> T. S. Hahm, *Phys. Fluids* **31**, 2670 (1988).
- <sup>7</sup> T. S. Hahm, W. W. Lee, and A. Brizard, *Phys. Fluids* **31**, 1940 (1988).
- <sup>8</sup> A. J. Brizard, *J. Plasma Phys.* **41**, 541 (1989).
- <sup>9</sup> A. J. Brizard, *Phys. Plasmas* **2**, 459 (1995).
- <sup>10</sup> T. S. Hahm, *Phys. Plasmas* **3**, 4658 (1996).
- <sup>11</sup> H. Sugama, *Phys. Plasmas* **7**, 466 (2000).
- <sup>12</sup> H. Qin and W. M. Tang, *Phys. Plasmas* **11**, 1052 (2004).
- <sup>13</sup> A. Brizard and T. S. Hahm, *Rev. Mod. Phys.* **79**, 421 (2007).
- <sup>14</sup> T. S. Hahm, Lu Wang, and J. Madsen, *Phys. Plasmas* **16**, 022305 (2009).
- <sup>15</sup> W. W. Lee, *Phys. Fluids* **26**, 556 (1983).
- <sup>16</sup> B. B. Kadomtsev and O. P. Pogutse, *Sov. Phys. JETP* **24**, 1172, (1967).
- <sup>17</sup> R. G. Littlejohn, *Phys. Scr.* **T2/1**, 119 (1982).
- <sup>18</sup> B. H. Fong and T. S. Hahm, *Phys. Plasmas* **6**, 188 (1999).
- <sup>19</sup> A. J. Brizard, *Phys. Plasmas* **7**, 3238 (2000).
- <sup>20</sup> L. Chen, R. L. Berger, J. G. Lominadze, M. N. Rosenbluth, and P. H. Rutherford, *Phys. Rev. Lett.* **39**, 754 (1977).
- <sup>21</sup> F. Y. Gang and P. H. Diamond, *Phys. Fluids B* **2**, 2976 (1990).
- <sup>22</sup> F. Y. Gang, P. H. Diamond, and M. N. Rosenbluth, *Phys. Fluids B* **3**, 68 (1991).
- <sup>23</sup> T. S. Hahm and W. M. Tang, *Phys. Fluids B* **3**, 989 (1991).

- <sup>24</sup> M. A. Beer and G. W. Hammett, *Phys. Plasmas*, **3**, 4018 (1996).
- <sup>25</sup> T. H. Stix, *Phys. Fluids* **16**, 1260 (1973).
- <sup>26</sup> F. L. Hinton and J. A. Robertson, *Phys. Fluids* **27**, 1243 (1984).
- <sup>27</sup> M. N. Rosenbluth and F. L. Hinton, *Phys. Rev. Lett.* **80**, 724 (1998).
- <sup>28</sup> F. L. Hinton and M. N. Rosenbluth, *Plasma Phys. Control. Fusion* **41**, A653 (1999).
- <sup>29</sup> A. M. Dimits, G. Bateman, M. A. Beer, et al., *Phys. Plasmas* **7**, 969 (2000).
- <sup>30</sup> E. A. Belli, Ph.D. dissertation, Princeton University, 2006.
- <sup>31</sup> E. A. Belli, G. W. Hammett, and W. Dorland, *Phys. Plasmas* **15**, 092303 (2008).
- <sup>32</sup> P. Angelino, X. Garbet, L. Villard, et al., *Phys. Plasmas* **15**, 062306 (2008).
- <sup>33</sup> Y. Xiao and P. J. Catto, *Phys. Plasmas* **13**, 082307 (2006).
- <sup>34</sup> H. Sugama and T.-H. Watanabe, *Phys. Plasmas* **13** 012501 (2006).
- <sup>35</sup> H. Sugama and T.-H. Watanabe, *Phys. Plasmas* **16** 056101 (2009).
- <sup>36</sup> T. S. Hahm, M. A. Beer, Z. Lin, G. W. Hammett, W. W. Lee, and W. M. Tang, *Phys. Plasmas* **9**, 922 (1999).
- <sup>37</sup> F. Jenko, W. Dorland, M. Kotschenreuther, and B. N. Rogers, *Phys. Plasmas* **7**, 1904 (2000).
- <sup>38</sup> Y. Xiao and P. J. Catto, *Phys. Plasmas* **13**, 102311 (2006).
- <sup>39</sup> P. J. Catto, *Plasma Phys.* **20**, 719 (1978).
- <sup>40</sup> A. Brizard, *Phys. Fluids B* **4**, 1213 (1992).
- <sup>41</sup> P. H. Diamond, S.-I. Itoh, K. Itoh, and T. S. Hahm, *Plasma Phys. Control. Fusion* **47**, R35 (2005).
- <sup>42</sup> E. J. Kim, C. Holland, and P. H. Diamond, *Phys. Rev. Lett.* **91**, 075003 (2003).
- <sup>43</sup> P. H. Diamond, M. N. Rosenbluth, F. L. Hinton, M. Malkov, J. Fleischer, and A. Smolyakov, IAEA-CN-69/TH3/1 (1998).
- <sup>44</sup> L. Chen, Z. Lin, and R. White, *Phys. Plasma* **7**, 3129 (2000).
- <sup>45</sup> Z. Lin, L. Chen, I. Holod, et al., IAEA-CN/TH/P2-8 (2006).
- <sup>46</sup> Y. Xiao and Z. Lin, submitted to *Phys. Rev. Lett.* (2009).

TABLE I: Derivation of nonlinear gyrokinetics (GK) and nonlinear bounce-kinetics (BK) using conventional multiple-scale-ordering expansion (Conventional) and Lie-transform perturbation methods (Modern).

	Conventional	Modern
GK	Frieman and Chen '82 <sup>1</sup>	Dubin '83 <sup>5</sup> , Hahm '88 <sup>6</sup> , Hahm et al., '88 <sup>7</sup> Brizard '89 <sup>8</sup> , Sugama '00 <sup>11</sup> , Qin et al., '04 <sup>12</sup>
BK	Kadomtsev et al., '67 <sup>16</sup> , Gang et al., '91 <sup>22</sup>	Littlejohn '82 <sup>3</sup> , Fong and Hahm '99 <sup>18</sup> Brizard '00 <sup>19</sup>

TABLE II: Derivation of classical polarization ( $n_{cl}$ ) and neoclassical polarization ( $n_{nc}$ ) via conventional and modern gyrokinetics and bounce-kinetics, which are denoted by CGK, MGK, CBK, and MBK; respectively.

	Lee '83 <sup>15</sup>	Dubin '83 <sup>5</sup> , Hahm '96 <sup>10</sup> Hahm et al., '09 <sup>14</sup>	Fong and Hahm '99 <sup>18</sup>	Rosenbluth and Hinton '98 <sup>27</sup> Sugama et. al., '06 <sup>34</sup> , Xiao '06 <sup>38</sup>	This work
$n_{cl}$	CGK	MGK		CGK	MGK
$n_{nc}$			MBK	CBK	MBK

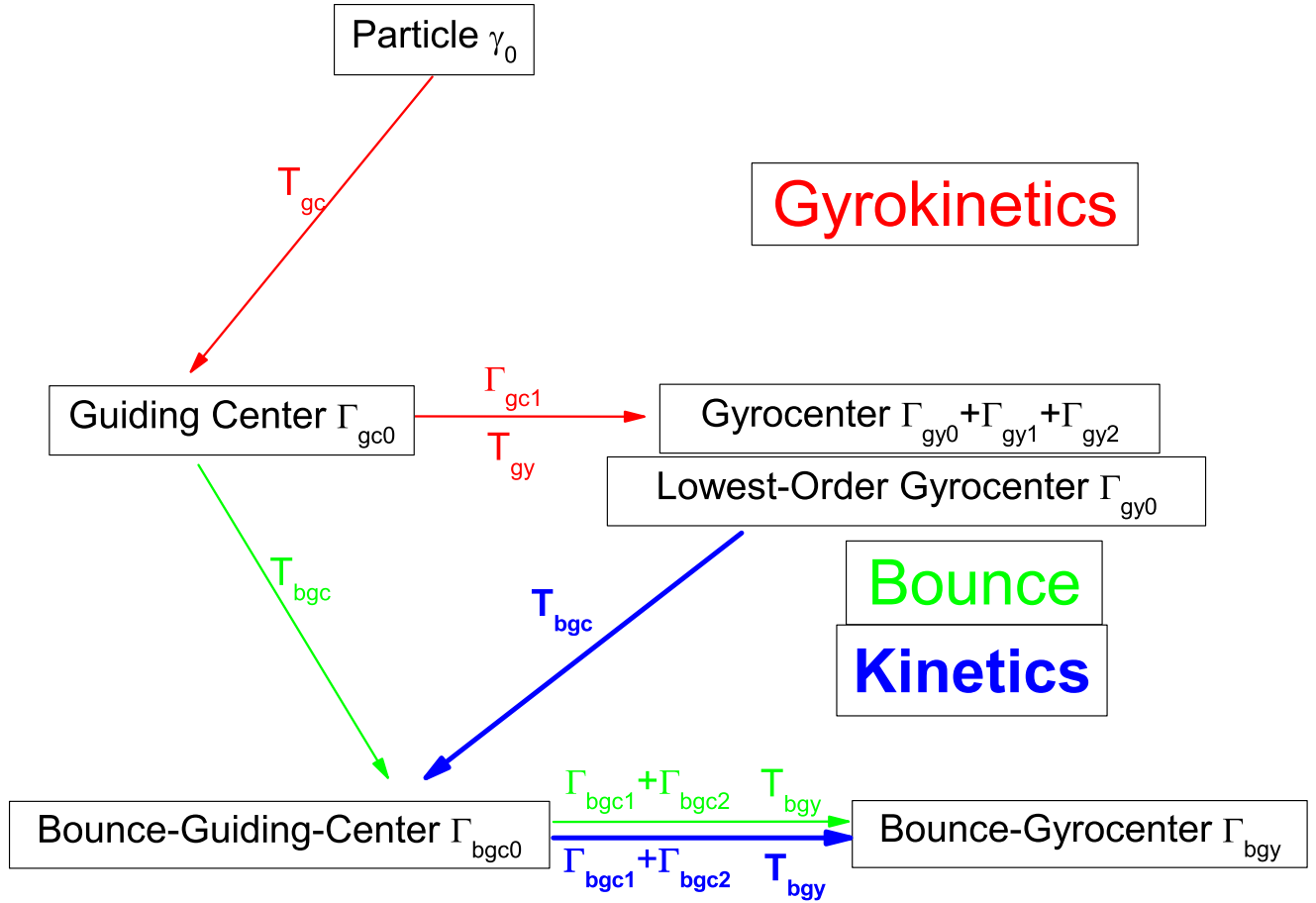


FIG. 1: The procedures of push-forward phase-space transformations for gyrokinetics and bounce-kinetics. The push-forward transformations in the works in the modern GK part of Table I correspond to the procedures in red color. Littlejohn's work<sup>17</sup> corresponds to the green  $T_{bgc}$ , Fong and Hahm<sup>18</sup> and Brizard<sup>19</sup>'s works correspond to the procedures in green color without the FLR effects (without  $\Gamma_{bgc2}$  in Ref. 18). This work includes both gyrokinetics corresponding to the procedures in red color and bounce-kinetics corresponding to the procedures in blue color with the FLR effects.

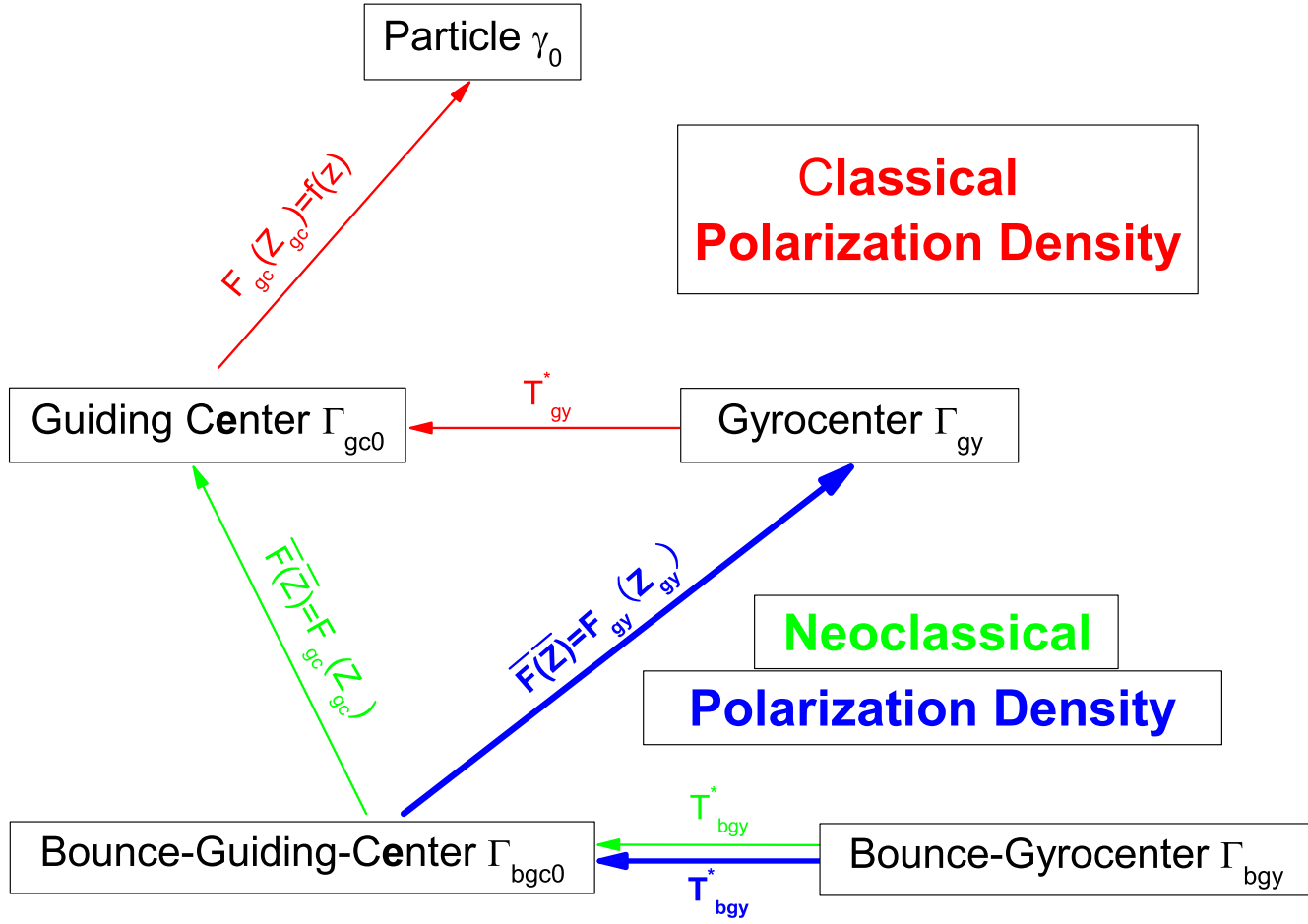


FIG. 2: The pull-back transformations to obtain the classical and neoclassical polarization densities. The classical polarization density in the works in the MGK part in Table II was obtained by the procedures in red color. Fong and Hahm's work<sup>18</sup> in MBK obtained the neoclassical polarization density by the procedures in green color in the long wavelength limit. This work obtains both the classical polarization density by the procedures in red color and the neoclassical polarization density by the procedures in blue color, for arbitrary wavelength.

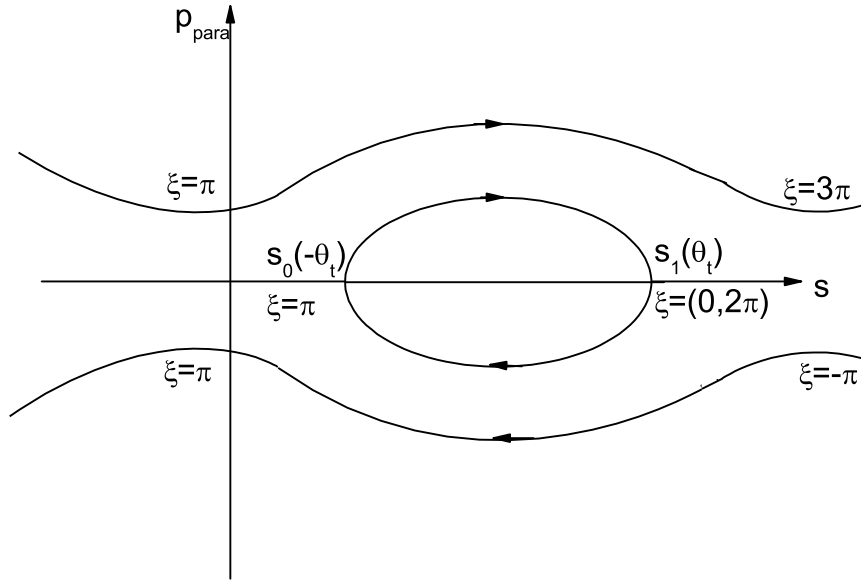


FIG. 3: The lowest-order bounce (transit) motion in  $(p_{\parallel}, s)$  phase plane. The closed orbit is for trapped particles, and the open lines for passing particles.

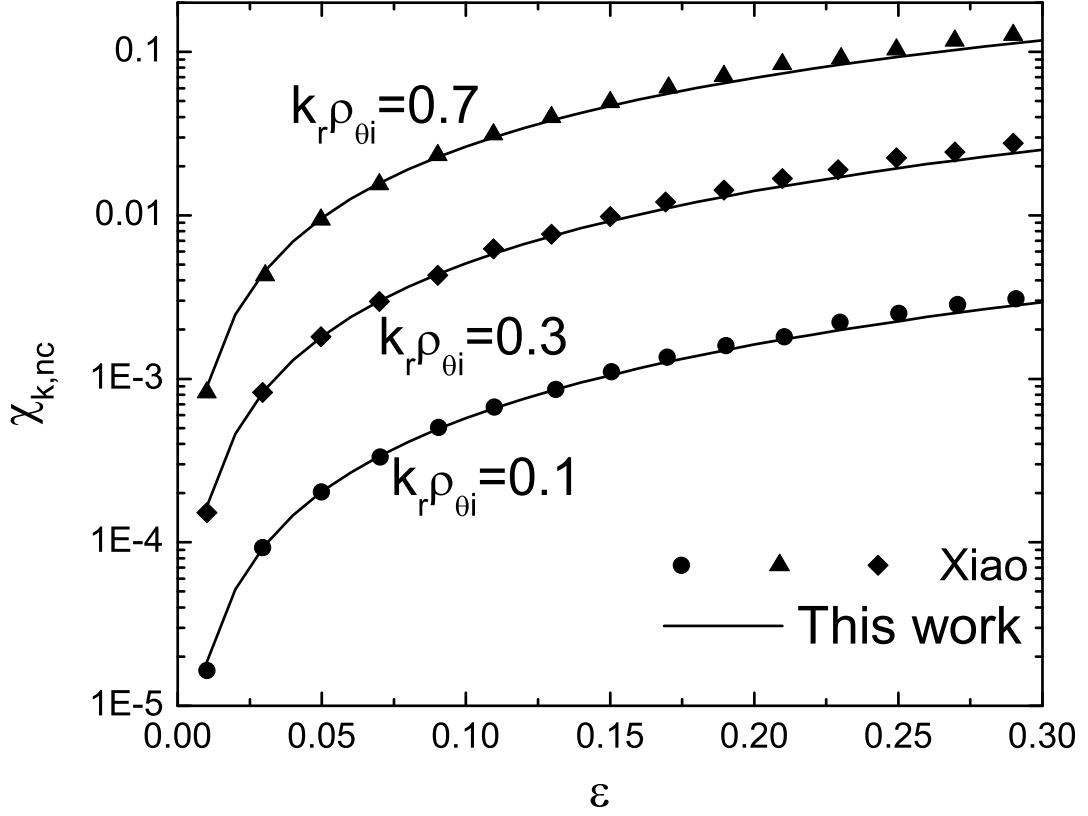


FIG. 4: The neoclassical susceptibility as a function of  $\epsilon$  for various radial wavelengths  $k_r \rho_{\theta i}$  and  $q = 1.4$ . The solid line represent our generalized neoclassical susceptibility from Eq. (51), and the discrete symbols represent the numerical results of Ref. 38.

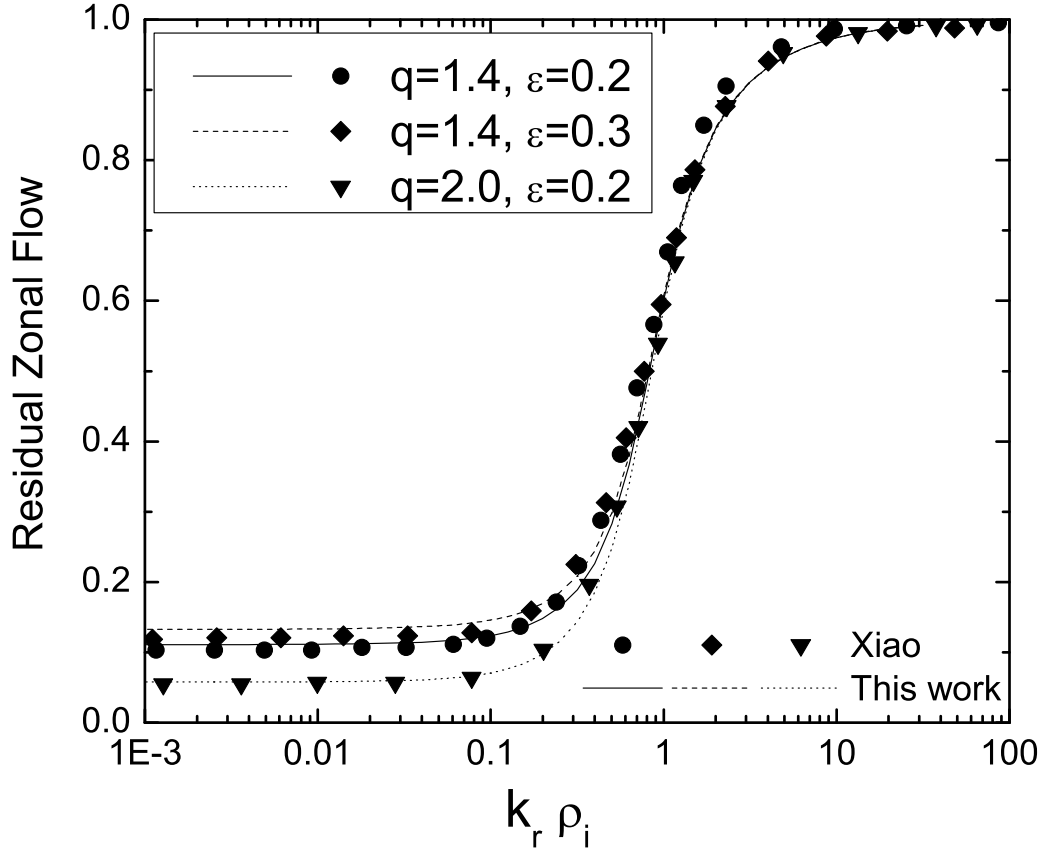


FIG. 5: The residual zonal flow level as a function of radial wavelength  $k_r \rho_i$ . Only ion polarization effect is included. The three lines are our analytical results, and the discrete symbols represent the numerical results of Ref. 38.

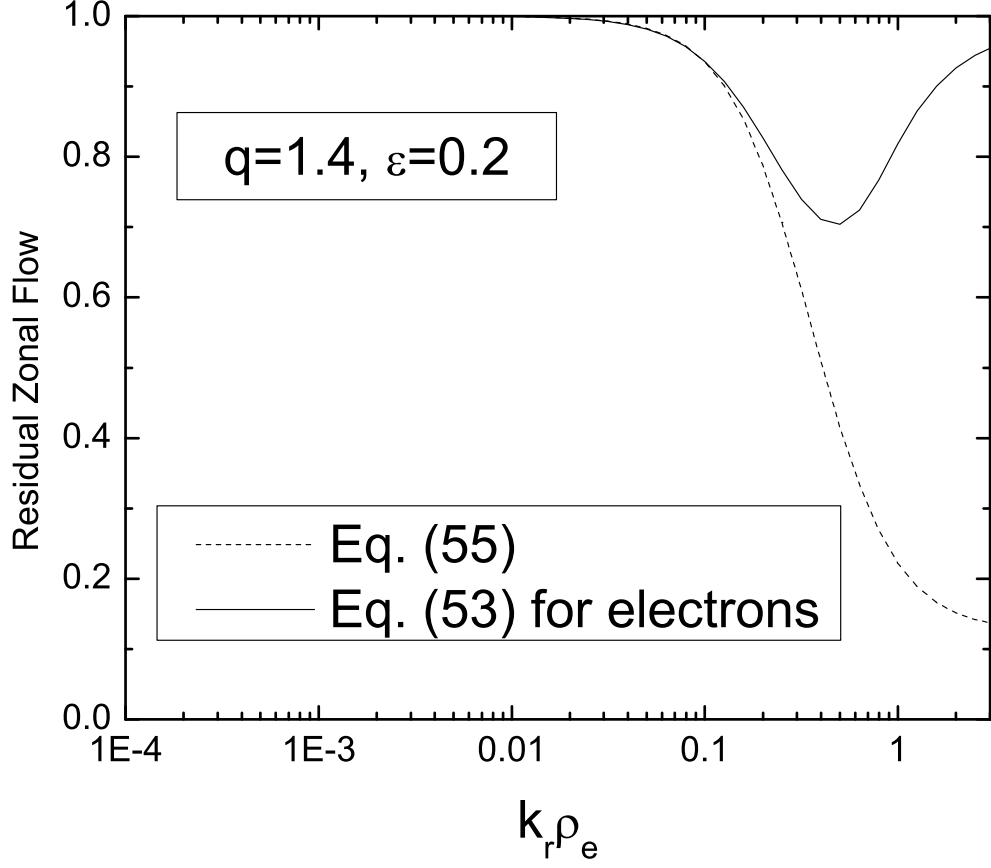


FIG. 6: The residual zonal flow level as a function of radial wavelength  $k_r \rho_e$  for adiabatic ions and  $\tau = 1$ . The dash line is from Eq. (55) which was presented as Eq. (8) in Ref. 42. The solid line represents the result based on Eq. (53) for electrons and adiabatic ions.

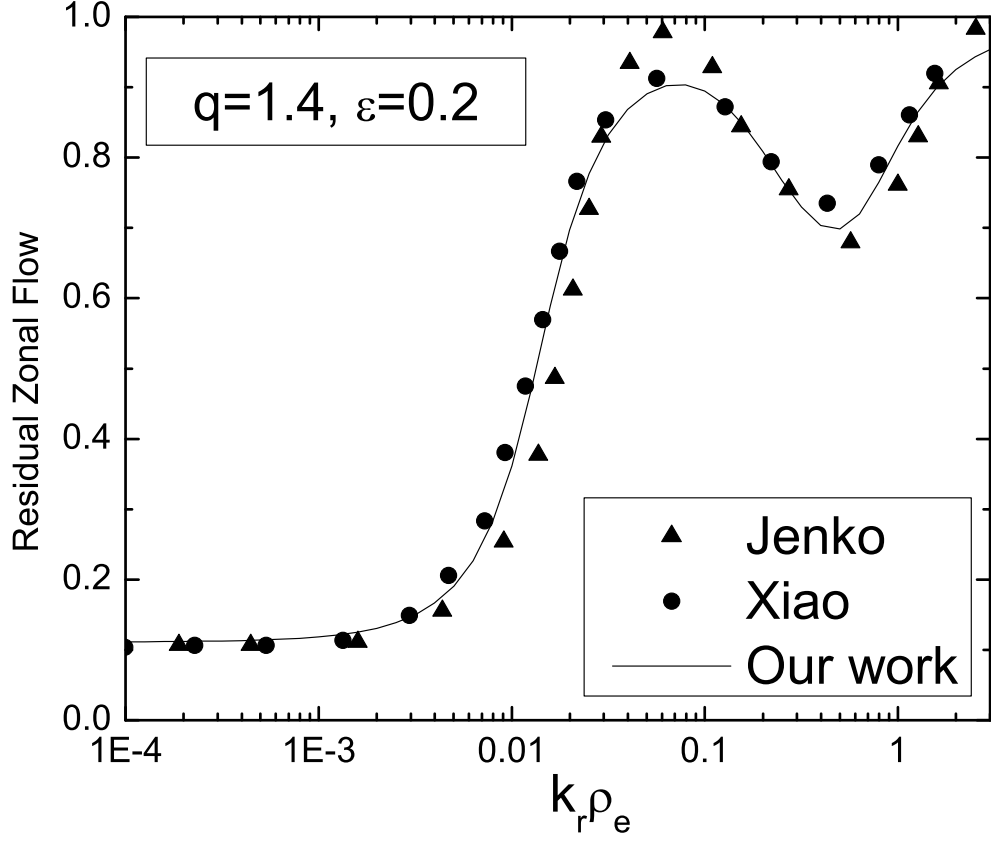


FIG. 7: The residual zonal flow level as a function of radial wavelength  $k_r \rho_e$  for  $\tau = 1$ . Both ion and electron polarization effects are included. The triangles are the simulation results of Ref. 37. The circles are the numerical result of Ref. 38 which have been converted from  $\rho_i$  to  $\rho_e$  for deuterium. The solid line represents our full analytical expression Eq. (53).

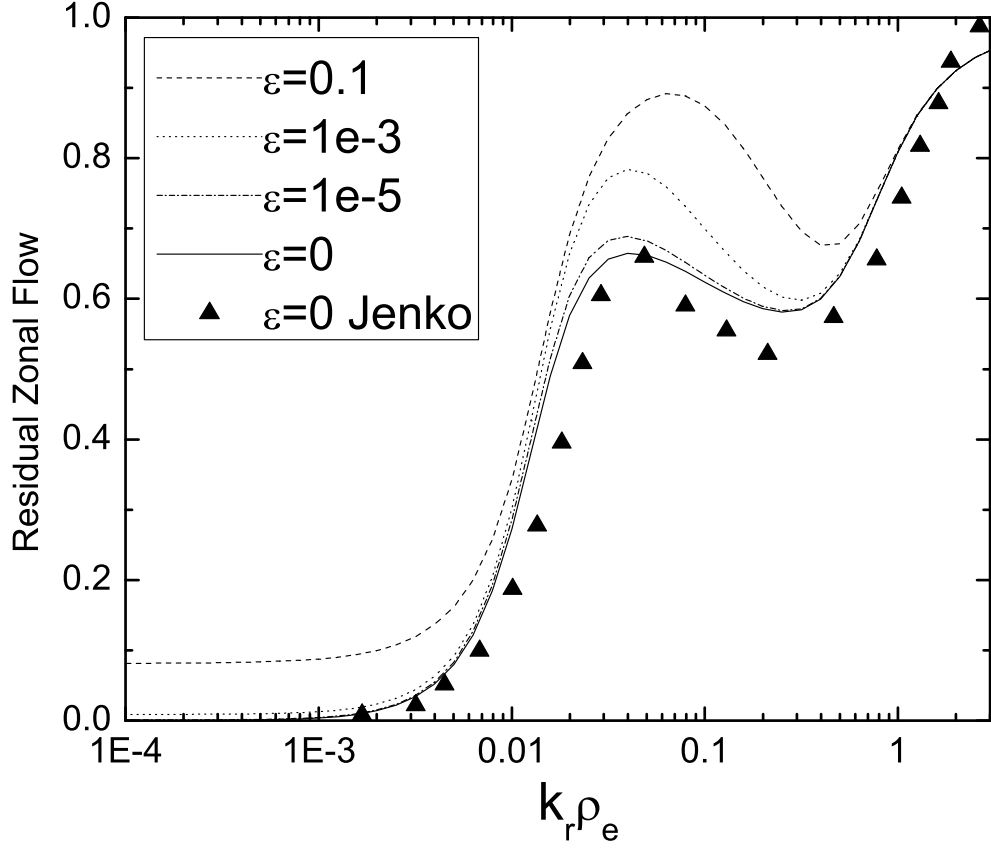


FIG. 8: The residual zonal flow level as a function of radial wavelength  $k_r \rho_e$  for  $\tau = 1$  and  $q = 1.4$ . Both ion and electron polarization effects are included. The four lines are our analytic results. The triangles represent the simulation results of Ref. 37.



The Princeton Plasma Physics Laboratory is operated  
by Princeton University under contract  
with the U.S. Department of Energy.

Information Services  
Princeton Plasma Physics Laboratory  
P.O. Box 451  
Princeton, NJ 08543

Phone: 609-243-2750  
Fax: 609-243-2751  
e-mail: [pppl\\_info@pppl.gov](mailto:pppl_info@pppl.gov)  
Internet Address: <http://www.pppl.gov>